

FIBER ARCHITECTURE AFFECTS FAILURE INITIATION AND ACCUMULATION AT THE FIBER-MATRIX INTERFACE

Minhao Zhou (1), Eric Neubauer Vickers (2), Grace D. O'Connell (1,3)

(1) Department of Mechanical Engineering
 University of California, Berkeley
 Berkeley, CA, United States

(2) Department of Molecular & Cell Biology
 University of California, Berkeley
 Berkeley, CA, United States

(3) Department of Orthopaedic Surgery
 University of California, San Francisco
 San Francisco, CA, United States

INTRODUCTION

Fiber-reinforced biological tissues withstand large, complex loads. Failure of these tissues can cause debilitating pain and reduced mobility. Understanding failure of tissues with limited self-healing capabilities, such as the annulus fibrosus or supraspinatus tendon, is pivotal as it may trigger catabolic remodeling, causing mechanical dysfunction.^{1,2}

Advancements in experimental methods and computational modeling facilitate investigations on subtissue level mechanics. Previous work showed that fiber sliding transmitted external loads and may prevent catastrophic tissue failure.³ Our recent experimental work quantified changes in tissue tensile properties from changes in biochemical compositions.⁴ We also developed and validated a multiscale, structure-based finite element model to study the fiber-matrix interactions at subtissue level.⁵

Preliminary work using the model demonstrated the potential role of stiffness gradients between fibers and the extrafibrillar matrix on subtissue damage mechanics, highlighting the importance of investigating the fiber-matrix interface. While hydration and fiber architecture are known to affect tissue subfailure mechanics,⁶⁻⁸ few studies have examined their effects on subtissue scale damage accumulation due to experimental limitations. Thus, the objective was to study the effect of hydration and fiber architecture on tissue failure mechanics by evaluating the effect of matrix swelling and fiber angle on subcomponent damage mechanics.

METHODS

Multiscale, structure-based models were developed to represent three-lamellae fiber-reinforced tissue specimens prepared for uniaxial tensile testing (Fig. 1A, 0.02 mm/lamella).⁵ A 0.01 mm-thick interfacial layer was incorporated to apply a stiffness gradient at the fiber-matrix interface (Fig. 1B-IL). The outer fiber layer and inner matrix layer (0.01 mm thick) was separated to analyze stress and strain at the fiber and

matrix periphery (Fig. 1B-a, b) separate from the inner fiber and exterior matrix material away from the interface (Fig. 1B-c, d).

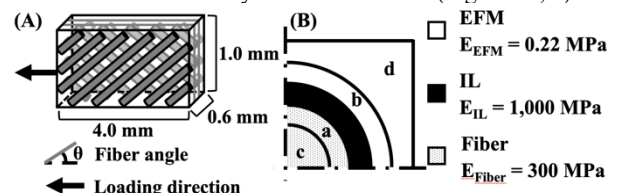


Figure 1: (A) Bulk tissue finite element model schematic. (B) Model setup at the fiber-matrix interface.

Tissue swelling was incorporated by using triphasic mixture theory and the extrafibrillar matrix (Fig. 1B-EFM) was defined as the subcomponent with active swelling capacity⁹. Fiber angle was defined with respect to the transverse plane (Fig. 1A-θ). Model A had a fixed charge density of -200 meq/g and fiber angle of ±45°, which was comparable to the inner annulus fibrosus (baseline). The effect of hydration was evaluated by varying EFM fixed charge density (FCD). Models B and C had an FCD of -150 and -100 meq/g, respectively, to represent the decrease in swelling capacity with degeneration. The effect of fiber orientation on fiber-matrix stress distributions was examined by varying fiber angle. Model D had a fiber angle of ±30° to represent fiber orientation of the outer annulus fibrosus tested along the circumferential direction and model E represented the fiber orientation of tendons or ligaments tested along the fiber direction.

Damage accumulation was evaluated using a strain-based reactive damage framework¹⁰. Based on preliminary work, IL modulus was defined to be greater than fiber modulus to prevent damage initiation and accumulation. Fiber, IL, and EFM moduli are summarized in Fig. 1B. All models were loaded in two steps: swelling in 0.15 M saline was followed by uniaxial tension to 25% bulk strain. The post-swelling, pre-

tension configuration was defined as the reference. Damage accumulation was assessed, and microscopic stress-strain profiles were evaluated at 15% bulk strain.

RESULTS

Tissue swelling decreased from ~40% for the baseline model (model *A*) to 13% for model *C* (-100 meq/g); however, hydration had a negligible effect on bulk tissue mechanics (Fig. 2-inset). As expected, bulk tissue modulus greatly increased as fibers became more aligned with the loading direction (Fig. 2).

Damage started to accumulate in baseline model *A* at ~15% bulk strain. A threefold decreased matrix swelling delayed damage initiation, resulting in a 50% decrease in accumulated damage by 20% bulk strain (Fig. 3-black vs. light blue bars); particularly, EFM and fiber damage were largely eliminated, while much of the damage occurred in IL.

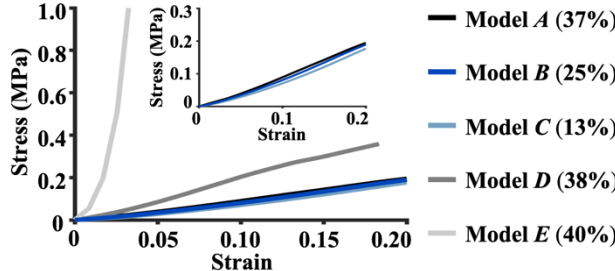


Figure 2: Bulk stress-strain response. Percentage value represents swelling ratio. Same color schematic is used in remaining figures.

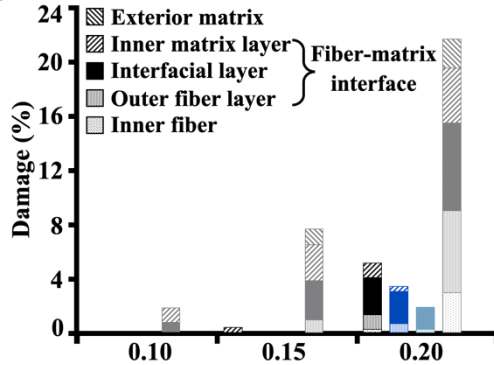


Figure 3: Tissue damage profiles at different bulk strains.

Large differences in damage accumulation behavior was observed with respect to fiber orientation. Model *D*, with an off-axis fiber angle of $\pm 30^\circ$, model *D* had the earliest damage initiation at $< 10\%$ bulk strain and the greatest damage accumulation. However, accumulated damage was reduced as fibers were either rotated away from or towards the loading direction ($\pm 45^\circ$, 0° in model *A*, *E*). Particularly, the overall accumulated damage found in model *D* was more than four times larger than model *A* (Fig. 3-dark gray vs. black bars) while no damage was observed in any subcomponents of model *E* (Fig. 3-no light gray bars).

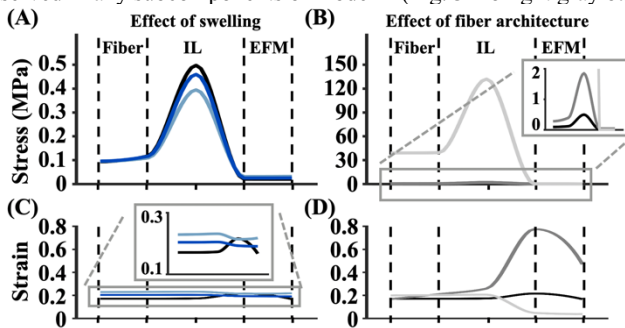


Figure 4: Tissue microscopic (A, B) stress & (C, D) strain profiles.

All models shared similar microscopic stress profile patterns, which increased from the Fiber/IL interface to mid-IL and then decreased towards the EFM/IL interface (Fig. 4A, B). Uniform stress profiles were observed in the fibers (~0.1 MPa) and EFM (~0.02 MPa), regardless of hydration level (Fig. 4A-Fiber, EFM). Compared to the baseline, a ~65% decrease in swelling resulted in a 20% decrease in the mid-IL peak stress (Fig. 4A-black vs. light blue line). Strain magnitudes were also relatively uniform throughout the tissue subcomponents regardless of swelling capacity (~0.2), but a decreased swelling ratio resulted in a shift in the location of peak strain from the IL/EFM interface to the mid-IL (Fig. 4C).

Fiber orientation greatly altered fiber and IL stress magnitude but did not change the pattern of the stress profile or EFM stress magnitude. In model *E* (0°), fiber and IL stress was more than 4X and 250X greater than the baseline model, respectively (Fig. 4B-light gray vs. black line). Significant differences in microscopic strain profiles were also observed with different fiber angles, especially between the mid-IL and EFM (Fig. 4D). Peak strains reached up to 0.8 for model *D* ($\pm 30^\circ$) at the IL/EFM interface, where microscopic strain was minimal for model *E*.

DISCUSSION

We used multiscale, structure-based finite element models to investigate the effect of hydration and fiber angle on damage accumulation at the fiber-matrix interface. Results presented here showed that both factors influenced tissue failure behavior, but fiber architecture had a greater effect. Our results also highlighted the importance of explicitly modeling tissue subcomponents when investigating failure propagation throughout the tissue.

The baseline model represented uniaxial tensile specimens prepared from the inner annulus fibrosus, where glycosaminoglycan content and, thus, matrix swelling capacity, decrease significantly with age and degeneration. Findings from this study showed that a reduced matrix swelling capacity resulted in little changes in bulk tissue mechanics, consistent with experimental observations of annulus fibrosus tensile properties in healthy and degenerated discs.¹¹

Replicating collagen fiber orientation and lamella architecture can be a manufacturing challenge for biological repair strategies. Fiber orientation in engineered intervertebral discs either have fibers aligns with the circumferential direction or at a fixed angle throughout the annulus.^{12,13} Damage initiated in the baseline model ($\pm 45^\circ$) at ~15% bulk strain; however, damage initiation and accumulation was highly sensitive to fiber orientation. When fibers were oriented at $\pm 30^\circ$, damage initiated earlier ($< 10\%$ bulk strain) and accumulated at a faster rate. Reducing the fiber angle to align with the loading direction eliminated damage accumulation in all tissue subcomponents; however, due to the highly anisotropic nature of the structure, damage accumulation would likely be much greater if the loading was applied along any other orientation.

The findings from this study show that both tissue hydration and fiber architecture affect subtissue level failure behavior, including damage initiation and accumulation. These observations are valuable for guiding biomimetic strategies aimed at designing hard-soft interfaces, as engineered tissues that result in greater localized stresses and strains may cause a catabolic remodeling cascade similar to degeneration. Moreover, this study provides additional information regarding the balance between tissue swelling and fiber architecture for maintain stress distributions,¹⁴ while limiting the risk for damage.

ACKNOWLEDGMENTS

NSF CMMI Grant No. 1760467

REFERENCES

- [1] Fucentese+, *J Bone Joint Surg Am*, 2012.
- [2] Adams+, *Spine*, 2006.
- [3] Vergari+, *Acta Biomater*, 2016.
- [4] Werbner+, *J Biomech*, 2019.
- [5] Zhou+, *BMMB*, 2019.
- [6] Ebara+, *Spine*, 1996.
- [7] Screen+, *Acta Biomaterialia*, 2006.
- [8] Han+, *Ann Biomed Eng*, 2012.
- [9] Lai+, *JBME*, 1991.
- [10] Nims+, *Interface Focus*, 2016.
- [11] O'Connell+, *J Biomech Eng*, 2009.
- [12] Bowles+, *Tissue Eng. Part A*, 2010.
- [13] Nerurkar+, *Spine*, 2010;
- [14] Yang & O'Connell, *Acta Biomaterialia*, 2019.